



HAL
open science

Isomer-dependent escape rate of xenon from a water-soluble cryptophane cage studied by Ab initio molecular dynamics

Rodolphe Pollet, Jean-Pierre Dognon, P. Berthault

► **To cite this version:**

Rodolphe Pollet, Jean-Pierre Dognon, P. Berthault. Isomer-dependent escape rate of xenon from a water-soluble cryptophane cage studied by Ab initio molecular dynamics. *ChemPhysChem*, 2023, 2023, pp.e202300509. 10.1002/cphc.202300509 . cea-04383667

HAL Id: cea-04383667

<https://cea.hal.science/cea-04383667v1>

Submitted on 9 Jan 2024

HAL is a multi-disciplinary open access archive for the deposit and dissemination of scientific research documents, whether they are published or not. The documents may come from teaching and research institutions in France or abroad, or from public or private research centers.

L'archive ouverte pluridisciplinaire **HAL**, est destinée au dépôt et à la diffusion de documents scientifiques de niveau recherche, publiés ou non, émanant des établissements d'enseignement et de recherche français ou étrangers, des laboratoires publics ou privés.



Distributed under a Creative Commons Attribution 4.0 International License

Isomer-Dependent Escape Rate of Xenon from a Water-Soluble Cryptophane Cage Studied by Ab Initio Molecular Dynamics

R. Pollet,^{✉[a]} J.-P. Dognon,^[a] and P. Berthault^[a]

The escape of xenon from the *anti* and *syn* diastereomers of hexacarboxylic-cryptophane-222 in water has been studied by ab initio molecular dynamics simulations. The structures of both complexes, when the xenon atom is trapped inside their cages, have been compared and show no major differences. The free-energy profiles corresponding to the escape reaction have been calculated with the Blue Moon ensemble method using the distance between Xe and the center of mass of the cage as the

reaction coordinate. The resulting free-energy barriers are very different; the escape rate is much faster in the case of the *syn* diastereomer, in agreement with experimental data obtained in hyperpolarized ¹²⁹Xe NMR. Our simulations reveal the mechanistic details for each diastereomer and provide an explanation for the different in-out xenon rates based on the solvation structure around the cages.

Introduction

A promising area of nuclear magnetic resonance molecular imaging uses hyperpolarized xenon, mainly produced via spin-exchange optical pumping. In this approach, the chemical shift of the noble gas varies drastically when it is encapsulated in dedicated host systems. These xenon hosts can be functionalized with ligands to target specific biological receptors,^[1] and this specific spectral signature enlightens the region of interest. The in-out xenon exchange rate is an important parameter as it determines the sensitivity of the method, this process enabling constant replenishment of the bound state in hyperpolarization and giving rise to detection approaches based on Chemical Exchange Saturation Transfer (CEST).^[2] Thus, understanding the processes that govern this dynamics is of high relevance.

Cryptophanes (Cr), organic cage-molecules made of two cyclotrimeratrylene bowls linked by alkoxy groups, are excellent candidates as such xenon hosts. Among all cryptophanes, the ability of water-soluble *anti*-Cr222(OCH₂COOH)₆, bearing three ethylenedioxy bridges together with six carboxylic functions (structure 1 in Figure 1), to efficiently and reversibly trap xenon in water was first established by Huber et al.^[3] From ¹H and ¹²⁹Xe nuclear magnetic resonance (NMR), the structure and dynamics of the host-guest complex were studied and an in-out xenon exchange rate of 3.2 s⁻¹ was roughly estimated at 289 K under a xenon pressure of 101 kPa. Later, this complex was shown to be a highly sensitive probe of the local pH and an exchange rate of 100 s⁻¹ was reported, however in different

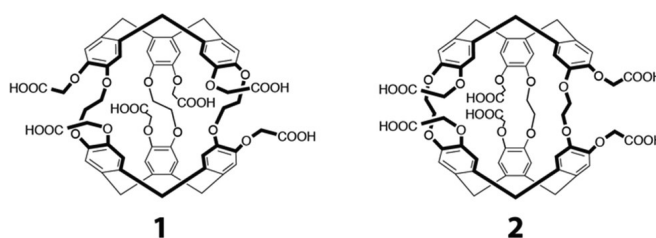


Figure 1. *Anti* (1) and *syn* (2) hexacarboxylic-cryptophane-222 (Cr-222) diastereomers.

experimental conditions.^[4] Actually, a “degenerate” or “kick-out” exchange, characterized by a xenon in-out rate depending on the host-guest concentration ratio, was demonstrated for this kind of molecular systems.^[5,6]

Recently, the *syn* diastereomer of this cryptophane (2 in Figure 1) was shown to induce faster xenon depolarization in CEST experiments than the *anti* diastereomer, under the same experimental conditions.^[7] The in-out exchange of xenon is faster, so its detectability is greater. Indeed the depolarization rate depends on the xenon escape rate according to:^[8,9]

$$\lambda_{on}(\omega_1) \approx f \cdot k_{out} \frac{\omega_1^2}{\omega_1^2 + k_{out}^2} \quad (1)$$

where ω_1 is the strength of the saturation applied at the resonance of the encapsulated xenon frequency, f is the fraction of encapsulated xenon, and k_{out} is the xenon out rate. So, with a sufficiently high saturation strength, the faster xenon leaves the host molecule the more effective the depolarization (and thus the detectability). The affinities of both diastereomers for xenon in aqueous solution being similar, the escape of xenon from *syn* was found to be approximately 6 times faster compared to *anti* at low cryptophane concentration in PBS (phosphate buffer saline).

[a] Dr. R. Pollet, Dr. J.-P. Dognon, Dr. P. Berthault
Université Paris-Saclay, CEA, CNRS, NIMBE, 91191, Gif-sur-Yvette, France
E-mail: rodolphe.pollet@cea.fr

© 2023 The Authors. ChemPhysChem published by Wiley-VCH GmbH. This is an open access article under the terms of the Creative Commons Attribution License, which permits use, distribution and reproduction in any medium, provided the original work is properly cited.

To explain these NMR results,^[7] atomic-scale calculations can shed light on the structure and thermodynamics of the Xe@cryptophane complexes. The less computational demanding, yet non-empirical, methods are based on density functional theory (DFT). Relativistic and solvation effects can also be incorporated for a better description of such complexes in solution, even if only an implicit solvent model is used.^[10] Higher-level calculations based on second-order Møller–Plesset perturbation theory (MP2) have shown that dispersion forces play a major role in the interaction between xenon and small Cr-111 cages.^[11] A comparison between several density functional approximations and MP2, using a continuum solvent model, has confirmed that dispersion-corrected density functionals are required to study these systems.^[12] As for the theoretical investigation of the decomplexation of xenon, the most accurate approach would therefore rely on ab initio molecular dynamics (AIMD) simulations^[13] with an explicit description of the solvent, the inclusion of relativistic effects through pseudopotentials, and a dispersion-corrected density functional. This is the approach retained in this work, which is the first AIMD simulation of a Xe@cryptophane complex in aqueous solution at finite temperature, focusing not only on its structure but also on the xenon in-out exchange. While the former can be studied with a conventional Car-Parrinello (CP) simulation,^[14] the free-energy barrier associated with the xenon escape reaction is so large in comparison to thermal fluctuations that an accelerated sampling technique is required to observe this rare event (see, e.g., a review of some available enhanced sampling methods).^[15] As such a technique, the Blue Moon method^[16] used in this work will be briefly described in the section.

Results and Discussion

Prior to the study of the escape of xenon from each cage, the structure and internal dynamics of each host-guest complex has been studied. During the unconstrained CP simulations, the same conformational change occurred for both diastereomers, namely one of the three ethylenedioxy bridges changed from a *gauche* to a *trans* conformation (see OCCO dihedral angles in Table 1). This event occurred after approximately 6 ps for *anti*

Table 1. Structures of *anti* (1) and *syn* (2) hexacarboxylic-cryptophane-222 (Cr-222) diastereomers encapsulating one xenon atom, from their unconstrained CP simulations at 300 K.

	<i>anti</i>	<i>syn</i>
trajectory length (ps)	39.5	13.8
OCCO angles (°) ^[a]	72 70 165	−87 71 182
diameter (Å) ^[b]	8.49 9.25 9.39	9.34 9.37 9.67
$d_{\text{Xe-CM}}$ (Å) ^[c]	0.69 (0.27)	0.64 (0.30)

[a] Dihedral angles of the three ethylenedioxy bridges. [b] Distances between corresponding CH₂ carbon atoms of the cyclotrimeratylene bowls. [c] Distance between xenon and the center of mass of the six crown CH₂ carbon atoms.

and 11 ps for *syn*. The size of each cavity can be gauged by calculating the averaged distances between opposite crown methylene bridges. As reported in Table 1, the diameter of the cavity appears slightly smaller in the case of the *anti* diastereomer. Another useful characteristic is the fluctuating position of xenon within the cavity, which can contribute to the observed chemical shift, as for example revealed by ab initio simulations of Xe@C₆₀.^[17] For (1), the averaged distance between xenon and the center of mass of all of the cryptophane atoms is 0.62 Å (or 0.69 Å for only the six crown methylene carbon atoms), which shows that the noble gas is not exactly located at the center of the cavity. These values are almost identical in the case of (2), with a corresponding averaged distance equal to 0.62 Å (or 0.64 Å for only the six carbon atoms). Overall, the previous structural data can not explain why the experimental xenon out rate is higher for the *syn* in comparison to the *anti* diastereomer.

The changes in free energy when xenon escapes the cage of conformers (1) and (2) as obtained by the Blue Moon ensemble method are plotted in Figure 2. The distance between xenon and the center of mass of the cage, $d_{\text{Xe-CM}}$, was gradually increased until the portal was passed and beyond. One can observe that both free energy profiles exhibit an almost continuous decrease from large (i.e., free xenon) to small (i.e., encapsulated xenon) distances, which means that the entrance of the atom inside the cage is almost barrierless. We also note that during all these simulations, no water molecule can be observed within the cavity; the cage remains empty when xenon crosses one portal. This is in contrast with a recent classical molecular dynamics study of bare Cr-222 (i.e., without solubility enhancing groups) where one or more H₂O molecules

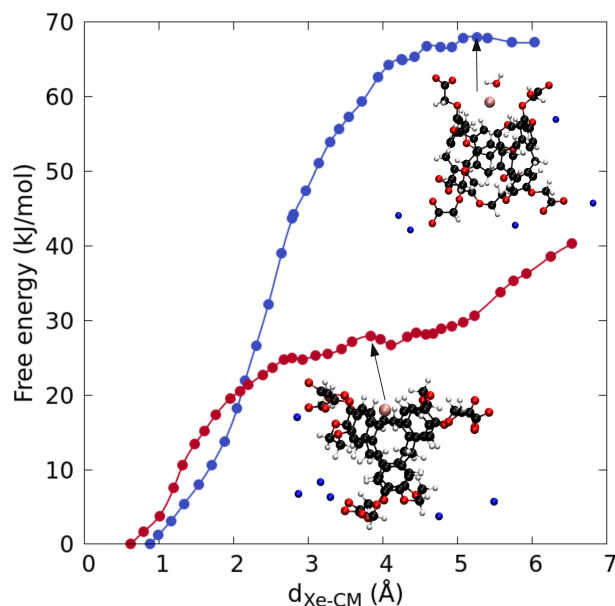


Figure 2. Free energy profiles of *anti* (1), in blue color, and *syn* (2), in red color, hexacarboxylic-cryptophane-222 (Cr-222) diastereomers from Blue Moon calculations at 300 K. Inset figures show typical configurations at the portal.

enter the cage, water being described as a catalyst for the escape of xenon.^[18]

For both diastereomers, this portal is located between a *gauche* and a *trans* conformations of ethylenedioxy bridges and the corresponding $d_{\text{Xe-CM}}^{\text{portal}}$ values are 5.26 Å for (1) and 3.83 Å for (2). The associated free-energy maxima are significantly different, namely 68 kJ/mol for *anti* and 27 kJ/mol for *syn*, which confirms that the xenon escape is significantly faster for the latter diastereomer. The different kinetics between the two complexes can first be rationalized by examining the average geometry at the portal. For (1), Xe is approximately in the plane defined by two ether oxygen atoms of two OCH₂COO⁻ groups (at 3.2 (0.1) and 3.3 (0.1) Å from Xe) and one water oxygen atom (at 3.6 (0.2) Å from Xe). For (2), Xe is approximately in the plane defined by two ether oxygen atoms of two OCH₂COO⁻ groups (at 3.6 (0.1) and 3.9 (0.3) Å from Xe) and one oxygen atom of the OCH₂CH₂O bridge in *trans* conformation (at 4.1 (0.2) Å from Xe). The mouth of the portal is therefore slightly more open and less rigid in the case of *syn*. Moreover, we observe an inversion of the *trans* OCH₂CH₂O bridge, namely the exchange between the two CH₂ groups, during the escape of xenon from (2). This inversion can be monitored by following the two C_{ph}OCC dihedral angles of the bridge, which for example change from -147/-68 to -63/-138° in less than 2 ps along an unconstrained trajectory starting from a structure where xenon is at the portal before returning to the encapsulated xenon configuration. In contrast, the escape from (1) is impeded by the presence of the water molecule mentioned above, which blocks the portal. With a rocking motion (i.e., the rotation around an axis perpendicular to the plane that contains its three atoms), this water molecule forms one or two hydrogen bonds with the two accepting OCH₂COO⁻ groups (see Figure 3), with average interatomic distances of 2.85 and 2.86 Å and HOH angles of 157 and 135°, respectively. As a consequence, the escape of Xe requires in this case the breaking of these two hydrogen bonds followed by the reorientation of the water molecule (no other hydrogen bond

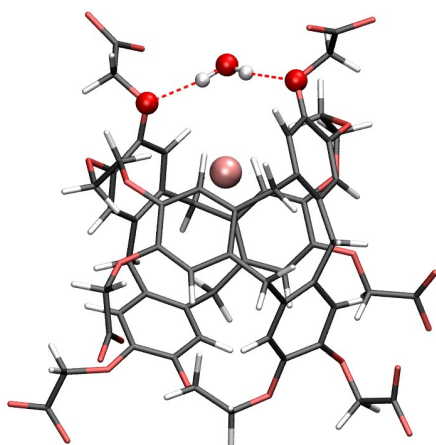


Figure 3. Typical configuration before xenon crosses the portal of *anti* (1) hexacarboxylic-cryptophane-222 (Cr-222) diastereomer with a water molecule on top.

needs to be broken since an initial donor water molecule detached from the blocking water during the last 16 ps of the unconstrained CP simulation). In fact, the analysis of the trajectories reveals very different distributions of the solvent molecules around the cryptophane. In the case of the *anti* diastereomer, the distribution is indeed rather homogeneous and spherical, with the two closest water molecules at 3.6 and 4.4 Å from Xe at the transition state. In contrast, the different orientation of the carboxylate groups in the *syn* diastereomer define a hydrophobic pocket outside the portal to be crossed by xenon. This empty space therefore provides an efficient pathway for the xenon escape, which mainly requires the inversion of the OCH₂CH₂O bridge (see above). Unfortunately, in the AIMD simulation this empty channel actually connects the chelate and its closest image due to the finite size of the periodic cell. As a consequence, configurations where xenon leaves this empty space to enter bulk water are out of reach with the present simulations. Further simulations with a larger computational box would be required to reconstruct the full free-energy profile for *syn* but the present simulations do provide the barrier corresponding to the escape of Xe from a portal of the cryptophane cage. However a quantitative comparison with experiment is therefore not straightforward for this diastereomer since the experimental rate corresponds to the reaction that leads to a fully hydrated xenon. For the *anti* diastereomer, the highest free-energy on the plateau observed at large distances, of 68 kJ/mol, approximately corresponds to a hundred of milliseconds (or $k_{\text{out}} \approx 9 \text{ s}^{-1}$) by using Eyring equation, which is in good agreement with NMR experiments.

Conclusions

The slightly different structures of both xenon complexes do not solely explain why the xenon escape from the *syn* diastereomer is experimentally faster compared to the *anti* one, unless their solvent distributions outside the portals are also compared. These distributions are indeed significantly different because of the orientations of the carboxylate arms, which give rise to specific free-energy pathways of xenon crossing the portals and different free-energy maxima. In the *anti* diastereomer, a water molecule is allowed to approach (but never penetrates, conversely to the result found in another theoretical study^[18]) and built a hydrogen-bonding bridge between two OCH₂COO⁻, which has to be broken for xenon to escape. Note that such an effect is mainly attributable to the presence of oxygen atoms on the aromatic rings in distinct geometries, and therefore such a difference in *syn-anti* behavior should be found on other cryptophanes with this characteristics. This is indeed the case for the Cr222(OH)₆ pair (results not shown). Similarly, the reduction of the xenon exchange dynamics due to the presence of water molecules near portals of cryptophanes with aromatic amine or amide groups was previously hypothesized owing to their ability to act as hydrogen-bond donors and acceptors.^[19] The exchange rate of xenon in novel encapsulating ligands could therefore be modulated with hydrogen-bonding networks formed between the functional groups and water

molecules as a crucial design parameter of better xenon biosensors.

The next stage of this theoretical study, which is underway in our laboratory, could consist in increasing the freely dissolved xenon concentration, which leads to the appearance of the so-called *kick-out* reaction (or degenerate exchange), where a freely dissolved xenon participates to the ejection of an encapsulated xenon atom.^[20] Depending on the complexity of the mechanism, the same Blue Moon ensemble or a more general accelerated sampling technique such as metadynamics could then be used.

Computational Details

The geometry of each diastereomer in their *gauche* conformation (i.e., with dihedral angles of the OCH₂CH₂O ethylenedioxy bridges equal to 60°) was initially optimized with the TURBOMOLE package^[21] at the B97-D3(BJ)^[22]/def2-TZVP level of theory using a small-core relativistic pseudopotential for Xe.^[23] The optimized complex was then solvated with the PACKMOL software,^[24] with 153 water molecules and six Na⁺ counterions in an orthorhombic box whose volume is approximately 8168 Å³ (see Figure 4).

The AIMD simulations were performed with the CPMD code (version 4.1),^[25] using the PBE exchange-correlation approximation^[26] corrected for dispersion effects (D2),^[27] with ultra-soft pseudopotentials^[28] including scalar relativistic effects and allowing a plane wave cutoff of only 30 Ry (for Xe, the 4*d* electrons were explicitly included in the valence). Although this corresponds to 76447 plane waves, which can be considered as a state-of-the-art calculation, the efficient hybrid parallelization of the CPMD code led to a performance of about 3 ps per day on nodes featuring two 64 core AMD EPYC processors running at 2.6 GHz. The initial CP trajectories used a fictitious electron mass of 700 a.u., a time step of 6 a.u., and Nosé–Hoover chain thermostats^[29] (with a chain length of three) both for ions (with the target temperature set to 300 K and thermostat frequency to 2500 cm⁻¹) and electrons in order to prevent heat transfer between both subsystems. In addition, hydrogen atoms were replaced by deuterium atoms to maintain adiabaticity. The atomic mass of Xe was set to its standard atomic

weight of 131.293 a.m.u. The time lengths of these initial CP trajectories are 39.5 ps and 13.8 ps for the *anti* (1) and *syn* (2) diastereomers in aqueous solution, respectively.

We used the Blue Moon ensemble^[16] to study the escape of xenon from the hexacarboxylate Cr-222 cavities. The distance $d_{\text{Xe-CM}}$ between xenon and the center of mass of each cavity was selected as the reaction coordinate to be sampled with a series of constrained AIMD simulations, assuming small deformations of the portals of the cavities. To this aim, a dummy atom was added at the center of mass of the coordinates of the six crown CH₂ carbon atoms of the two cyclotrimeratrylene (CTV) bowls. The length of each constrained MD simulation was approximately 2.5 ps including a relaxation of approximately 1 ps. The change in free energy along the $d_{\text{Xe-CM}}$ reaction coordinate was eventually obtained by numerically integrating the time-averaged force of constraint along the reaction path.

Acknowledgements

This work was granted access to the HPC resources of TGCC under the allocations 2021-A0100811468 and 2022-AD010811468R1 made by GENCI. The authors warmly thank Thierry Brotin and his team for giving them access to these water-soluble cryptophanes. These require meticulous synthesis, which is perfectly mastered at ENS Lyon.

Conflict of Interests

There are no conflicts of interest to declare.

Data Availability Statement

The data that support the findings of this study are available in the supplementary material of this article.

Keywords: ab initio calculations · host-guest systems · molecular dynamics · xenon

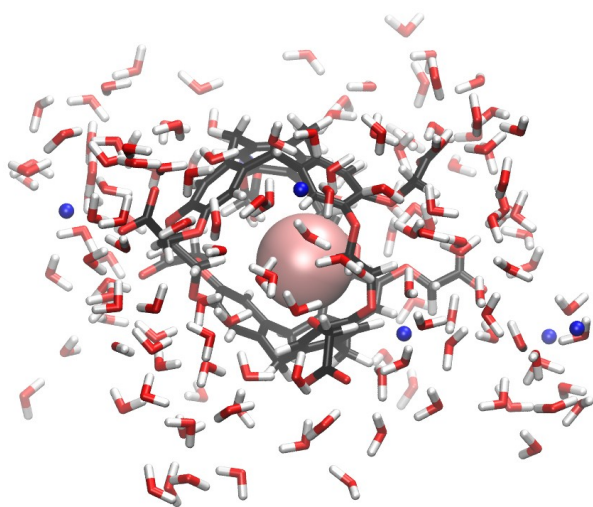


Figure 4. Host-guest complex (1) solvated by 153 water molecules with six Na⁺ counterions (in CPK blue). Xenon in van der Waals representation.

- [1] P. Berthault, G. Huber, H. Desvaux, *Prog. Nucl. Magn. Reson. Spectrosc.* **2009**, *55*, 35.
- [2] L. Schröder, T. J. Lowery, C. Hilty, D. E. Wemmer, A. Pines, *Science* **2006**, *314*, 446.
- [3] G. Huber, T. Brotin, L. Dubois, H. Desvaux, J.-P. Dutasta, P. Berthault, *J. Am. Chem. Soc.* **2006**, *128*, 6239, pMID: 16669694.
- [4] P. Berthault, H. Desvaux, T. Wendlinger, M. Gyejacquot, A. Stopin, T. Brotin, J.-P. Dutasta, Y. Boulard, *Chemistry A European Journal* **2010**, *16*, 12941.
- [5] G. Huber, L. Beguin, H. Desvaux, T. Brotin, H. A. Fogarty, J.-P. Dutasta, P. Berthault, *J. Phys. Chem. A* **2008**, *112*, 11363, pMID: 18925727.
- [6] S. Korchak, W. Kilian, L. Mitschang, *Chem. Commun.* **2015**, *51*, 1721.
- [7] E. Léonce, T. Brotin, P. Berthault, *Phys. Chem. Chem. Phys.* **2022**, *24*, 24793.
- [8] M. Zaiss, M. Schnurr, P. Bachert, *J. Chem. Phys.* **2012**, *136*, 144106.
- [9] M. Kunth, C. Witte, L. Schröder, *J. Chem. Phys.* **2014**, *141*, 194202.
- [10] A. Bagno, G. Saielli, *Chemistry A European Journal* **2012**, *18*, 7341.
- [11] E. Dubost, J.-P. Dognon, B. Rousseau, G. Milanole, C. Dugave, Y. Boulard, E. Léonce, C. Boutin, P. Berthault, *Angew. Chem. Int. Ed.* **2014**, *53*, 9837.
- [12] T. B. Demissie, K. Ruud, J. H. Hansen, *J. Phys. Chem. A* **2017**, *121*, 9669, pMID: 29178799.

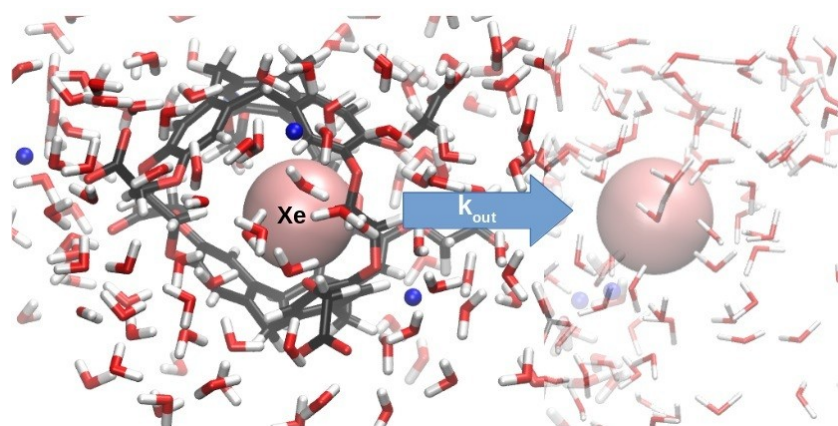
- [13] D. Marx, J. Hutter, *Ab initio Molecular Dynamics: Basic Theory and Advanced Methods*, Cambridge University Press, Cambridge 2009.
- [14] R. Car, M. Parrinello, *Phys. Rev. Lett.* **1985**, *55*, 2471.
- [15] C. Abrams, G. Bussi, *Entropy* **2014**, *16*, 163.
- [16] M. Sprik, G. Ciccotti, *J. Chem. Phys.* **1998**, *109*, 7737.
- [17] M. Straka, P. Lantto, J. Vaara, *J. Phys. Chem. A* **2008**, *112*, 2658, pMID: 18303877.
- [18] P. Hilla, J. Vaara, *Phys. Chem. Chem. Phys.* **2022**, *24*, 17946.
- [19] M. Doll, P. Berthault, E. Léonce, C. Boutin, E. Jeanneau, T. Brotin, N. De Rycke, *J. Org. Chem.* **2022**, *87*, 2912, pMID: 35080182.
- [20] S. Korchak, W. Kilian, L. Mitschang, *Chem. Commun.* **2015**, *51*, 1721.
- [21] TURBOMOLE V7.1 2016, a development of University of Karlsruhe and Forschungszentrum Karlsruhe GmbH, 1989–2007, TURBOMOLE GmbH, since 2007; available from <http://www.turbomole.com>.
- [22] S. Grimme, J. Antony, S. Ehrlich, H. Krieg, *J. Chem. Phys.* **2010**, *132*, 154104.
- [23] K. A. Peterson, D. Figgen, E. Goll, H. Stoll, M. Dolg, *J. Chem. Phys.* **2003**, *119*, 11113.
- [24] L. Martinez, R. Andrade, E. G. Birgin, J. M. Martinez, *J. Comput. Chem.* **2009**, *30*, 2157.
- [25] CPMD, <http://www.cpmc.org/>, Copyright IBM Corp 1990–2019, Copyright MPI für Festkörperforschung Stuttgart 1997–2001.
- [26] J. P. Perdew, K. Burke, M. Ernzerhof, *Phys. Rev. Lett.* **1996**, *77*, 3865, Erratum: *Phys Rev Lett* **1997**, *78*, 1396.
- [27] S. Grimme, *J. Comput. Chem.* **2006**, *27*, 1787.
- [28] D. Vanderbilt, *Phys. Rev. B* **1990**, *41*, 7892.
- [29] G. J. Martyna, M. L. Klein, M. Tuckerman, *J. Chem. Phys.* **1992**, *97*, 2635.

Manuscript received: July 21, 2023

Revised manuscript received: October 31, 2023

Accepted manuscript online: October 31, 2023

Version of record online: ■■, ■■



Comparative study of the complexes of two cryptophane diastereomers with xenon via accelerated methods of ab-initio molecular dynamics reveals totally distinctive behavior for

the escape of xenon from the cages, thereby explaining their difference in detectability through hyperpolarized ^{129}Xe NMR.

*Dr. R. Pollet**, *Dr. J.-P. Dognon*, *Dr. P. Berthault*

1 – 6

Isomer-Dependent Escape Rate of Xenon from a Water-Soluble Cryptophane Cage Studied by Ab Initio Molecular Dynamics